Nomarski serial time-encoded amplified microscopy for high-speed contrast-enhanced imaging of transparent media

Ali M. Fard,[1,2,*] Ata Mahjoubfar,[1,2] Keisuke Goda,[1,2,3] Daniel R. Gossett,[2,3] Dino Di Carlo,[2,3] and Bahram Jalali[1,2,3,4]

[1]*Department of Electrical Engineering, University of California, 420 Westwood Plaza, Los Angeles, CA 90095, USA*
[2]*California NanoSystems Institute, University of California, 570 Westwood Plaza, Los Angeles, CA 90095, USA*
[3]*Department of Bioengineering, University of California, 420 Westwood Plaza, Los Angeles, CA 90095, USA*
[4]*Department of Surgery, David Geffen School of Medicine, University of California, 20 Medical Plaza, Los Angeles, CA 90095, USA*
*ali.fard@ucla.edu

Abstract: High-speed high-contrast imaging modalities that enable image acquisition of transparent media without the need for chemical staining are essential tools for a broad range of applications; from semiconductor process monitoring to blood screening. Here we introduce a method for contrast-enhanced imaging of unstained transparent objects that is capable of high-throughput imaging. This method combines the Nomarski phase contrast capability with the ultrahigh frame rate and shutter speed of serial time-encoded amplified microscopy. As a proof of concept, we show imaging of a transparent test structure and white blood cells in flow at a shutter speed of 33 ps and a frame rate of 36.1 MHz using a single-pixel photo-detector. This method is expected to be a valuable tool for high-throughput screening of unstained cells.

OCIS codes: (180.3170) Interference microscopy; (320.7160) Ultrafast technology; (110.0180) Microscopy.

References and Links

1. D. Murphy, "Differential interference contrast (DIC) microscopy and modulation contrast microscopy," in *Fundamentals of Light Microscopy and Digital Imaging* (Wiley-Liss, New York, 2001).
2. E. Salmon and P. Tran, "High-resolution video-enhanced differential interference contrast (VEDIC) light microscope," in *Video Microscopy*, G. Sluder and D. Wolf, eds. (Academic, New York, 1998).
3. H. Ishiwata, M. Itoh, and T. Yatagai, "A new method of three-dimensional measurement by differential interference contrast microscope," Opt. Commun. **260**(1), 117–126 (2006).
4. E. B. Van Munster, E. K. Winter, and J. A. Aten, "Measurement-based evaluation of optical pathlength distributions reconstructed from simulated differential interference contrast images," J. Microsc. **191**(2), 170–176 (1998).
5. J. Götze, "Application of Nomarski DIC and cathodoluminescence (CL) microscopy to building materials," Mater. Charact. **60**(7), 594–602 (2009).
6. M. Sokabe and F. Sachs, "The structure and dynamics of patch-clamped membranes: a study using differential interference contrast light microscopy," J. Cell Biol. **111**(2), 599–606 (1990).
7. D. J. Stephens and V. J. Allan, "Light microscopy techniques for live cell imaging," Science **300**(5616), 82–86 (2003).
8. G. Verheyen, E. Crabbé, H. Joris, and A. Van Steirteghem, "Simple and reliable identification of the human round spermatid by inverted phase-contrast microscopy," Hum. Reprod. **13**(6), 1570–1577 (1998).
9. C. L. Curl, T. Harris, P. J. Harris, B. E. Allman, C. J. Bellair, A. G. Stewart, and L. M. D. Delbridge, "Quantitative phase microscopy: a new tool for measurement of cell culture growth and confluency in situ," Pflugers Arch. **448**(4), 462–468 (2004).
10. M. G. Coulthard, A. Nelson, T. Smith, and J. D. Perry, "Point-of-care diagnostic tests for childhood urinary-tract infection: phase-contrast microscopy for bacteria, stick testing, and counting white blood cells," J. Clin. Pathol. **63**(9), 823–829 (2010).
11. H. Petty, "High speed microscopy in biomedical research," Opt. Photonics News **15**, 40–45 (2004).
12. K. Goda, K. K. Tsia, and B. Jalali, "Serial time-encoded amplified imaging for real-time observation of fast dynamic phenomena," Nature **458**(7242), 1145–1149 (2009).

13. B. Jalali, P. Soon-Shiong, and K. Goda, "Breaking speed and sensitivity limits," Optik Photonik **5**(2), 32–36 (2010).
14. S. Chatterjee, "Design considerations and fabrication techniques of Nomarski reflection microscope," Opt. Eng. **42**(8), 2202–2213 (2003).
15. C. C. Montarou and T. K. Gaylord, "Analysis and design of modified Wollaston prisms," Appl. Opt. **38**(31), 6604–6616 (1999).
16. K. Goda, D. R. Solli, K. K. Tsia, and B. Jalali, "Theory of amplified dispersive Fourier transformation," Phys. Rev. A **80**(4), 043821 (2009).
17. D. R. Solli, J. Chou, and B. Jalali, "Amplified wavelength–time transformation for real-time spectroscopy," Nat. Photonics **2**(1), 48–51 (2008).
18. J. Chou, O. Boyraz, D. R. Solli, and B. Jalali, "Femtosecond real-time single-shot digitizer," Appl. Phys. Lett. **91**(16), 161105 (2007).
19. K. Goda, A. Motafakker-Fard, and B. Jalali, "Phase-contrast serial time-encoded amplified microscopy," in *CLEO/Europe and EQEC 2009 Conference Digest* (Optical Society of America, 2009), paper CH3_4.
20. D. Di Carlo, "Inertial microfluidics," Lab Chip **9**(21), 3038–3046 (2009).
21. D. Di Carlo, D. Irimia, R. G. Tompkins, and M. Toner, "Continuous inertial focusing, ordering, and separation of particles in microchannels," Proc. Natl. Acad. Sci. U.S.A. **104**(48), 18892–18897 (2007).
22. D. L. Lessor, J. S. Hartman, and R. L. Gordon, "Quantitative surface topography determination by Nomarski reflection microscopy," J. Opt. Soc. Am. **69**(2), 357–366 (1979).
23. K. K. Tsia, K. Goda, D. Capewell, and B. Jalali, "Performance of serial time-encoded amplified microscope," Opt. Express **18**(10), 10016–10028 (2010).

1. Introduction

Optical imaging is widely used for detection, inspection, and diagnostics in numerous industrial, biomedical, and scientific applications. In particular, imaging modalities, such as differential interference contrast (DIC) microscopy [1,2] and phase-contrast (PC) microscopy [2], which can capture images of transparent objects without the need for chemical staining, are of a significant importance. Metallurgy and semiconductor processing heavily rely on these modalities for imaging surface scratches, lines and edges, defects, and contaminations inside the material being tested [3–5]. Also, such modalities play a crucial role in detection and diagnostics of diseased cells (e.g., leukemia) in advanced biomedical research and clinical settings [6–9].

High-throughput imaging in such applications is highly desirable [10], but extremely challenging. For instance, high-throughput screening of biological cells (that show nearly no contrast with respect to their aqueous surroundings) enables finding of rare diseased cells in a large population of healthy cells. However, conventional techniques (e.g., DIC microscopy) with the ability to perform this task have relied on CCD (charge-coupled device) and CMOS (complementary metal-oxide-semiconductor) image sensors [11]. Hence, their image acquisition throughput is limited by that of CCD and CMOS cameras. More importantly, the shutter speed of even the fastest cameras is too slow, resulting in significant blurring of images during high-speed screening. Due to these technological limitations, conventional DIC and PC microscopy have not been commonly used for applications that require monitoring of dynamic samples in real time with high throughput.

The recently introduced imaging technology known as serial time-encoded amplified imaging or microscopy (STEAM) [12] overcomes limitations in conventional imaging and provides ~1000 times higher frame rates and shutter speeds than conventional image sensors. STEAM employs an amplified space-to-time mapping technique to encode the spatial information of an object into a one-dimensional (1D) serial time-domain optical waveform and optically amplify the image, simultaneously. The high-speed capability of the STEAM imager enables its use for applications in which high-throughput screening of an object is of interest, such as blood cell screening [13]. Unfortunately, the STEAM imager is inadequate for imaging of transparent objects but rather limited to opaque samples or samples with high refractive-index or absorption contrast. While the objects (e.g. biological cells) can be stained with dyes to increase their contrast, chemical staining requires time-consuming sample preparation and is often accompanied by cell death.

Here we present a method that overcomes the contrast limitation of STEAM and hence performs high-speed contrast-enhanced imaging of transparent media without the need for chemical staining. The presented technique, which we refer to as Nomarski serial time-

encoded amplified microscopy (N-STEAM) combines STEAM's high-speed capability and DIC/Nomarski microscopy's ability to image unstained transparent objects. To demonstrate our method, we show contrast enhancement in imaging of a transparent refractive-index-modulated structure and white blood cells in flow with 33 ps dwell time (shutter speed) at 36.1 MHz frame rate using a single-pixel photodetector. This method is expected to be a valuable tool for high-throughput screening and sorting of unstained cells.

2. Working principle of N-STEAM

N-STEAM is a DIC implementation of STEAM that obtains a differential phase contrast image of the object with very fast shutter speed and high frame rates. The N-STEAM employs a Nomarski prism (also known as modified Wollaston prism) [14,15] and spatial light dispersers (e.g., a pair of diffraction gratings) to produce two 1D spatially-dispersed orthogonally-polarized beams as illustrated in Fig. 1(a). It, then, illuminates two adjacent points on the object with each wavelength component but different polarizations. The illumination beams travel through the two incident points on the transparent object and hence, they experience different phase shifts associated with the optical path lengths (i.e., the product of the refractive index and thickness) of the two incident points on the object [Fig. 1(b)]. By recombining the two phase-encoded beams using the same Nomarski prism, the differential phase information is converted into an intensity modulation. In other words, the optical path length difference between the two incident points results in constructive/deconstructive interference for each wavelength. The image-encoded spectrum [Fig. 1(b)] is then converted into a temporal data stream, stretched in time, and simultaneously amplified using an amplified dispersive Fourier transformation [16–18]. The time stretch allows the image to be digitized by a conventional electronic digitizer. Also, the optical image amplification (~20 dB) over a wide optical bandwidth (as large as 60 nm) overcomes the loss of signal at high frame rates and is a key feature of this method. The temporal waveform in Fig. 1(c) indicates the repetitive pulses (corresponding to the line scans) detected by a single-pixel photodetector and illustrates the operation of N-STEAM at 36.1 MHz frame rate. In other words, N-STEAM's real-time capture of time-domain pulses enables pulse-to-pulse (frame-by-frame) image acquisition at 36.1 MHz rate.

A phase contrast implementation of the STEAM imager based on Hilbert transform has been reported by us before [19]. In that implementation, which does not use the Nomarski technique, the time domain signal is upconverted to a higher modulation frequency; therefore, the requirements on the speed of the digitizer is more demanding, and digital signal processing is required to perform the Hilbert transform. The present Nomarski based technique does not have such requirements.

3. N-STEAM implementation

In an implementation of N-STEAM, the broadband pulse laser is a mode-locked laser with a center wavelength of 1560 nm and a pulse repetition rate of 36.1 MHz. A highly nonlinear fiber and optical band-pass filter following the laser produces a train of pulses with ~20 nm bandwidth centered at 1591 nm as an illumination beam. Using a pair of diffraction gratings with 1100 lines/mm groove density, the pulses are spatially-dispersed into a 1D rainbow pattern enabling 1D line-scanning of the object. The 1D spatially-dispersed beam (i.e., 1D rainbow) is sent to a half-wave plate and a polarizer to rotate the polarization state of the light and ensure 45-degree linear polarization incident on the Nomarski prism. The Nomarski prism splits the illumination beam into two orthogonally-polarized 1D rainbow patterns (0 and 90 degrees).

The design of the Nomarski prism and the subsequent optics are such that the two orthogonally-polarized beams are incident on the object in the direction normal to the direction of the line scan. A mirror is placed at the back of the object to return the phase-encoded beams to the same optics, which results in double passing of the illumination beams through the object, and hence, doubles the phase shifts. After recombining the phase-encoded
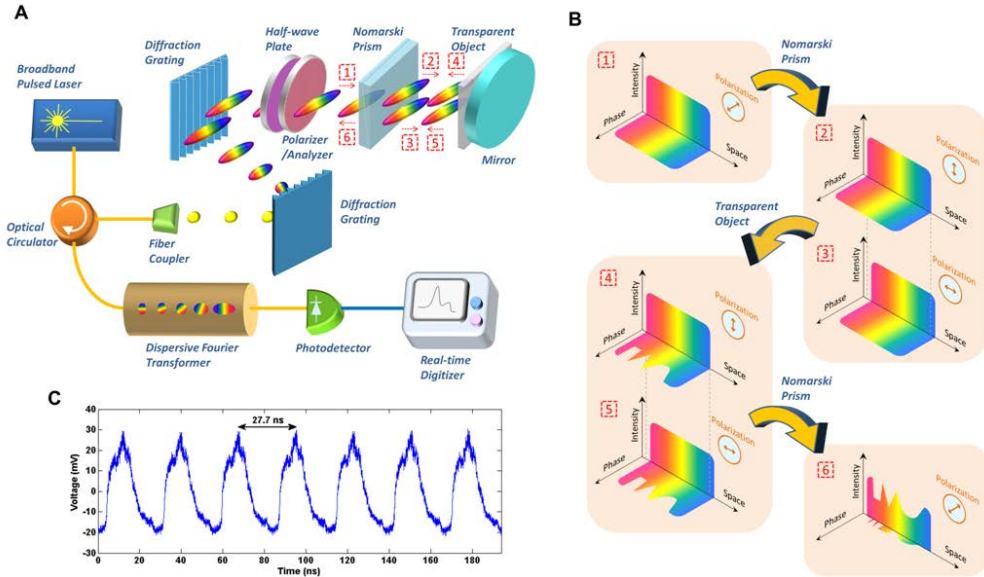
Fig. 1. Nomarski serial time-encoded amplified microscopy (N-STEAM). N-STEAM builds on a unique combination of STEAM's high-speed imaging capability and DIC/Nomarski microscopy's ability to image transparent objects without staining. (a) Schematic of the N-STEAM imager. The N-STEAM uses a Nomarski prism to encode the optical path length (the product of the refractive index and thickness) of the object into the optical spectrum of the illumination beam. (b) Evolution of the intensity, phase, and polarization of the illumination beam(s) at different points in the system. (c) Temporal waveform that shows N-STEAM's frames (line scans) at 36.1 MHz, corresponding to a repetition period of 27.7 ns.

beams using the same Nomarski prism, the spectrally-encoded beam is directed to a spool of optically-pumped dispersive fiber (with dispersion value of −1373 ps/nm) via an optical circulator to perform amplified dispersive Fourier transformation (gain of ~20dB). The time-encoded optical pulses are then captured by a high-speed photodetector with 10 GHz bandwidth and digitized by a real-time digitizer with 16 GHz bandwidth and 50 GS/s sampling rate (Tektronix – DPO71604). Digital signal processing including background and noise removal is performed offline to reconstruct the image of the object under test.

4. Results

To demonstrate our method, we performed imaging of a transparent structure using N-STEAM. The object is a transparent material with a periodic refractive-index modulation [i.e., a transmission grating with a groove density of 70 lines per millimeter, Fig. 2(a)]. Figures 2(b) and 2(c) compare the reconstructed two-dimensional (2D) images with N-STEAM and STEAM, respectively. The second dimension of the images was obtained by translating the object in the direction orthogonal to that of the line scans. The design of the object is such that the refractive-index modulation is small; hence, the reflection from different points on the object is below the sensitivity of the STEAM imager. With the Nomarski prism, the system provides differential phase-contrast in imaging of the object [Fig. 2(b)]. The captured image without the Nomarski prism (i.e., using STEAM without DIC implementation) shows the normalized reflectivity map of the object [Fig. 2(c)]. As evident from the images, significant contrast-enhancement is achieved by using N-STEAM. The high-intensity lines in the image are ~14 μm apart, which agrees with the specifications of the transparent structure.

In order to demonstrate the use of our method in high-speed high-contrast imaging of unstained biological cells and tissue, we also performed imaging of fast-flowing unstained white blood cells in a microfluidic channel [20,21]. White blood cells were isolated from
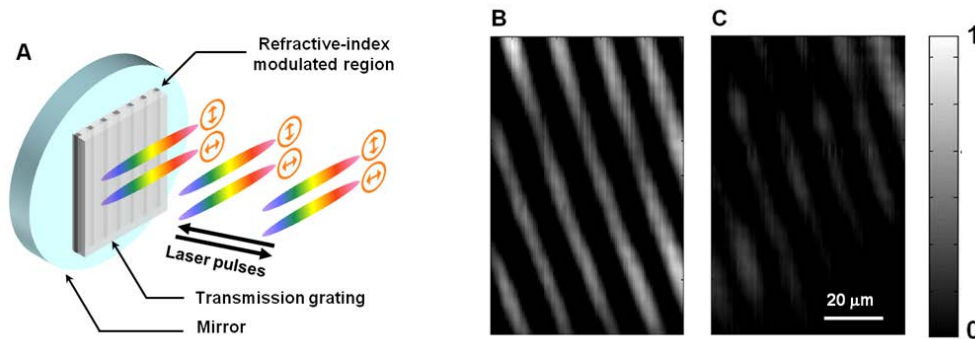
Fig. 2. (a) Schematic of the transparent refractive-index modulated structure aligned with the illumination beams. Images of a transparent refractive-index modulated structure captured using N-STEAM with (b) and without (c) the Nomarski prism. The imager without the prism is equivalent to STEAM, while the enhancement in the image contrast was obtained with the Nomarski prism (i.e., N-STEAM). The second dimension of the images was obtained by translating the sample in the direction normal to the line scans. The comparison of the images indicates significant contrast enhancement obtained by the N-STEAM.
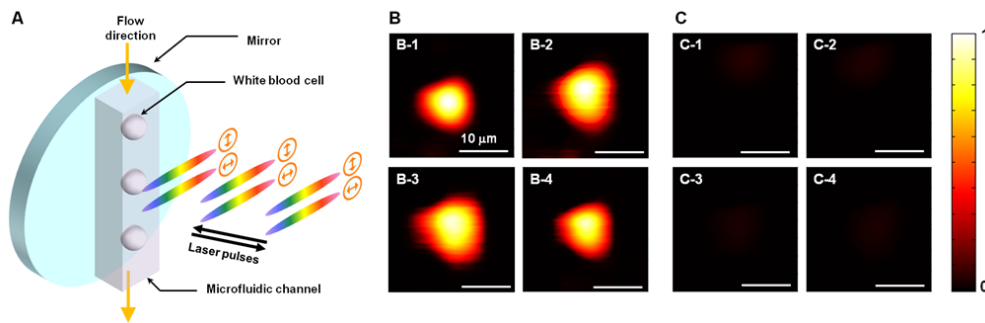

Fig. 3. (a) Schematic of the microfluidic channel aligned with respect to 1-D rainbow illumination pulses. Images of unstained white blood cells captured by N-STEAM, (b) with and, (c) without the Nomarski prism. The flow rate was 1 meter/s. The image contrasts obtained by N-STEAM is >15 times larger than those of obtained by STEAM. The rest of scale bars, 10μm.

whole blood by hypotonic lysis of red blood cells and resuspended in phosphate buffered saline. To acquire 2D images of the cells, they flow [Fig. 3(a)] at a flow speed of 1 meter/s in the direction orthogonal to that of the line scans – providing 400-500 image pixels in the flow direction for each white blood cell. Figures 3(b) and 3(c) compare the images of white blood cells captured by N-STEAM and STEAM, respectively. The image captured by N-STEAM [Fig. 3(b)] is based on the relative phase shift between the illumination beams when propagating through the cell, while the image captured by STEAM [Fig. 3(c)] shows the reflection from the surface of the cell. Note that the color coding in Fig. 3(b) represents the normalized optical path length of the cell, while that in Fig. 3(c) represents the normalized reflectivity of the cell. Interestingly, the image contrasts of the white blood cells captured by N-STEAM is >15 times higher than those of captured by STEAM; that is equivalent to ~12-dB signal-to-noise ratio (SNR) improvement over STEAM. This is due to poor refractive-index contrast and/or absorption of unstained white blood cells compared to their aqueous surrounding (i.e., phosphate buffered saline). Since N-STEAM reveals the optical path length of the cell (i.e., the product of refractive index and size), it can be potentially used to distinguish different types of cells that are similar in size, and hence suggests a path to high-throughput imaging-based cell analysis.

5. Discussions

5.1. Contrast enhancement

The N-STEAM's enhanced image-contrast can be obtained as follows. It can be adjusted using the offset phase shift between the two spatially-dispersed orthogonally-polarized beams. Similar to the expression derived in Ref. [22]. for conventional DIC or Nomarski microscopy, the intensity of each wavelength component of the interfered beam in N-STEAM is obtained by the expression,

$$I = I_0 \left[a_1 + a_2 \left(1 - \cos \chi \right) \right], \tag{1}$$

where $a_1 = \cos^2(\varphi_A - \varphi_P)$ and $a_2 = -0.5 \sin(2\varphi_A)\sin(2\varphi_P)$. Here φ_A and φ_P are the angles of the analyzer and polarizer, respectively, and χ is the differential phase shift between the two polarized beams. In N-STEAM, the polarizer and analyzer are the same as illustrated in Fig. 1(a); hence, φ_A and φ_P are equal to 45 degrees. The differential phase shift (χ) is composed of two parts: the phase shift offset and the phase shift due to the optical path length difference between the incident points on the object to be imaged. The phase shift offset is a constant phase shift due to different optical paths travelled by the two spatially-dispersed beams. This can be adjusted by changing the tilt angle of the prism with respect to the propagation direction of the illumination beam.

5.2. Specifications

The specification of N-STEAM demonstrated here is evaluated as follows. The number of image pixels is found to be N = $|D| \cdot \Delta\lambda \cdot f_{dig}$ = 1373, where D is the total dispersion in the dispersive fiber (D = −1373 ps/nm), $\Delta\lambda$ is the optical bandwidth ($\Delta\lambda$ = 20 nm), and f_{dig} is the sampling rate of the digitizer (f_{dig} = 50 GS/s). The diffraction-limited spatial resolution [23] is determined to be d $\approx\lambda$/2/NA $\approx$2 μm, where λ is the operation wavelength (λ = 1591 nm) and NA is the numerical aperture of the objective lens (NA = 0.4). The number of resolvable spectral points is estimated to be ~180 from the spectral resolution of the ADFT process [23]. Hence, the dwell time (shutter speed) is found to be ~33 ps from the bandwidth of each subpulse or wavelength component (20 nm / 180) in the line scan. The current implementation of the N-STEAM provides a 1D line-scan width of 100 μm; this has been validated using a known target (Resolution test target, Thorlabs, R2L2S1N).

6. Conclusion

We have proposed and demonstrated a method that enables high-speed contrast-enhanced image acquisition of transparent objects without the need for chemical staining. This imaging modality, N-STEAM, fills the contrast and speed gap between phase imaging-based techniques and STEAM imager. It couples the high-speed capability of the STEAM imager and differential phase contrast imaging of DIC / Nomarski microscopy. As the proof of concept, we performed imaging of a transparent structure and white blood cells in flow at 33 ps shutter speed and 36.1 MHz frame rate. N-STEAM holds promise for high-throughput imaging of unstained biological cells.

Acknowledgments